

This article was downloaded by:

On: 25 January 2011

Access details: *Access Details: Free Access*

Publisher *Taylor & Francis*

Informa Ltd Registered in England and Wales Registered Number: 1072954 Registered office: Mortimer House, 37-41 Mortimer Street, London W1T 3JH, UK



Liquid Crystals

Publication details, including instructions for authors and subscription information:

<http://www.informaworld.com/smpp/title~content=t713926090>

Influence of fluorine substituent on the mesomorphic properties of five-ring ester banana-shaped molecules

R. Amaranatha Reddy^a; B. K. Sadashiva Corresponding author^a

^a Raman Research Institute, C. V. Raman Avenue Sadashivanagar, Bangalore 560 080, India

Online publication date: 19 May 2010

To cite this Article Reddy, R. Amaranatha and Sadashiva Corresponding author, B. K.(2003) 'Influence of fluorine substituent on the mesomorphic properties of five-ring ester banana-shaped molecules', *Liquid Crystals*, 30: 9, 1031 – 1050

To link to this Article: DOI: 10.1080/0267829031000152978

URL: <http://dx.doi.org/10.1080/0267829031000152978>

PLEASE SCROLL DOWN FOR ARTICLE

Full terms and conditions of use: <http://www.informaworld.com/terms-and-conditions-of-access.pdf>

This article may be used for research, teaching and private study purposes. Any substantial or systematic reproduction, re-distribution, re-selling, loan or sub-licensing, systematic supply or distribution in any form to anyone is expressly forbidden.

The publisher does not give any warranty express or implied or make any representation that the contents will be complete or accurate or up to date. The accuracy of any instructions, formulae and drug doses should be independently verified with primary sources. The publisher shall not be liable for any loss, actions, claims, proceedings, demand or costs or damages whatsoever or howsoever caused arising directly or indirectly in connection with or arising out of the use of this material.

Influence of fluorine substituent on the mesomorphic properties of five-ring ester banana-shaped molecules

R. AMARANATHA REDDY and B. K. SADASHIVA*

Raman Research Institute, C. V. Raman Avenue Sadashivanagar,
Bangalore 560 080, India

(Received 31 January 2003; accepted 27 April 2003)

The synthesis and characterization of more than a hundred achiral compounds composed of banana-shaped molecules and belonging to eleven different homologous series are reported. All these symmetrical five-ring compounds are esters and are derived from resorcinol. The compounds have been systematically substituted by fluorine on the phenyl rings of the arms of these banana-shaped molecules. The mesophases exhibited by these compounds have been characterized using a combination of polarized light optical microscopy, differential scanning calorimetry and X-ray diffraction studies. Electro-optical investigations have been carried out on several compounds and both ferroelectric and antiferroelectric properties are observed. The influence of the position of the fluorine substituent on the nature of the mesophase obtained has been examined.

1. Introduction

The new sub-field of thermotropic liquid crystals involving the study of compounds composed of banana-shaped molecules, has provided a wealth of new and exciting mesophases in a short time. Over the last few years, a large number of such compounds have been synthesized with a view to understanding the relationship between molecular structure and the nature of the mesophase/s exhibited. These include compounds with five, six and seven aromatic rings in the core and have formed the basis of an excellent review [1]. Most of these compounds contain five aromatic rings with azomethine linking groups and are derivatives of resorcinol, which has been widely used as the central unit. The synthesis and characterization of mesophases obtained for complete homologous series of five-ring bent-core compounds appears to be limited [1, 2, 3]. There are a number of five-ring bent-core compounds in which the central phenyl ring is substituted by different groups [1, 4–13] and the influence of these groups on the mesomorphic properties has been studied. In addition, there are numerous studies on the effect of different lateral substituents on the arms of the five-ring bent-core molecules on the mesomorphic properties [14–19]. Amongst these, a lateral fluorine substituent *ortho* to the terminal *n*-alkoxy chain induces interesting electro-optical switching properties to the mesophases. For example, Bedel *et al.* [18, 19] reported ferroelectric switching

behaviour for the higher homologues of a few series of five-ring Schiff's base esters. Later, Nadasi *et al.* [20] found ferroelectric properties in achiral five-ring Schiff's base esters with lateral fluorine substituents on the central phenyl ring as well as on the outer phenyl rings. We demonstrated bistable switching characteristics for two different mesophases exhibited by two homologues of a series of five-ring esters containing fluorine substituents on the outer phenyl rings [21]. Recently, Rauch *et al.* [22] reported a ferroelectric phase for 3,4'-biphenylene-bis[4-(3-fluoro-4-*n*-octyloxyphenyl)iminomethyl]benzoate], which again contains fluorine substituent *ortho* to the terminal *n*-alkoxy chain. However, there has been no systematic evaluation of the influence of a lateral substituent on the liquid crystalline properties of compounds composed of banana-shaped molecules. It is for this reason that we decided to examine a system in detail.

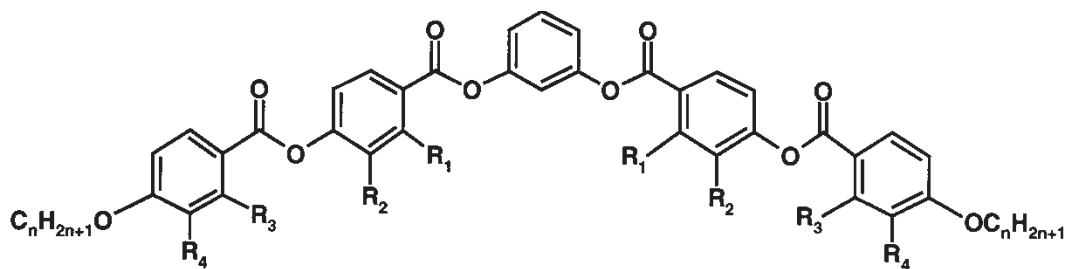
We chose a five-ring ester system derived from resorcinol which does not contain the relatively unstable azomethine linking group. We have systematically substituted the phenyl rings of the arms of the bent-core molecules with fluorine and examined the mesomorphic properties. A total of 101 compounds belonging to 11 different homologous series have been studied; these are shown in figure 1.

2. Experimental

2.1. Synthesis

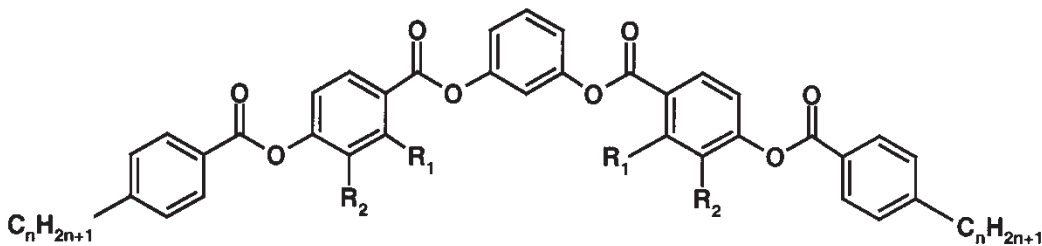
Several homologous series of compounds laterally fluoro-substituted on the arms of the symmetrical

*Author for correspondence; e-mail: sadashiv@rri.res.in



$n=1,2,3,\dots,12,14,16,18,20$

| | |
|------------------------------|-------------|
| $R_1=H, R_2=H, R_3=H, R_4=H$ | Series I |
| $R_1=F, R_2=H, R_3=H, R_4=H$ | Series II |
| $R_1=H, R_2=F, R_3=H, R_4=H$ | Series III |
| $R_1=H, R_2=H, R_3=F, R_4=H$ | Series IV |
| $R_1=H, R_2=H, R_3=H, R_4=F$ | Series V |
| $R_1=F, R_2=H, R_3=F, R_4=H$ | Series VI |
| $R_1=F, R_2=H, R_3=H, R_4=F$ | Series VII |
| $R_1=H, R_2=F, R_3=F, R_4=H$ | Series VIII |
| $R_1=H, R_2=F, R_3=H, R_4=F$ | Series IX |



$R_1=F, R_2=H,$ Series X

$n=8,9,10,11,12,14,16$

$R_1=H, R_2=F,$ Series XI

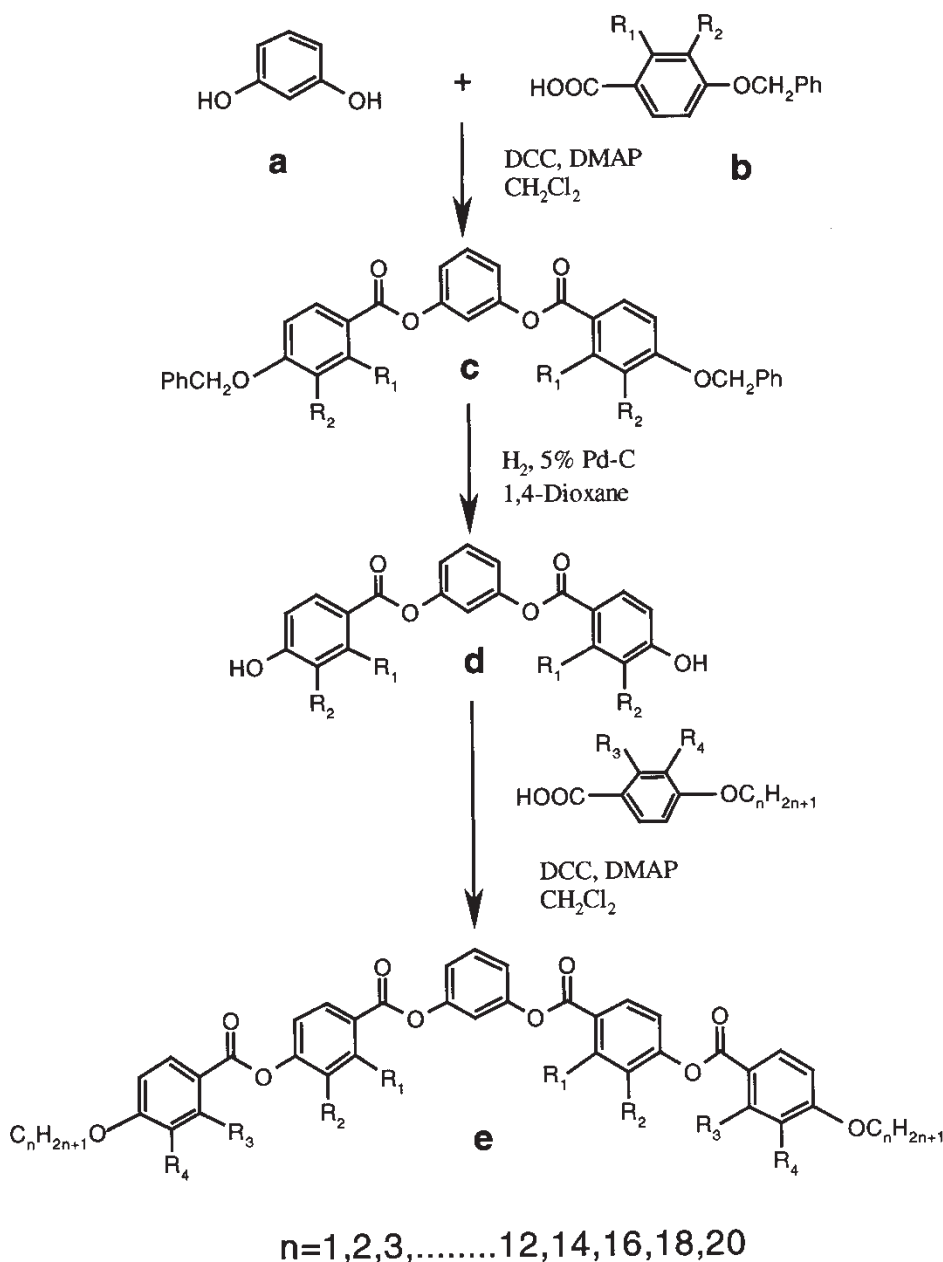
$n=14$

Figure 1. The general bent-core structures indicating the different homologous series.

bent-core (BC) molecules were synthesized by following the general synthetic pathway shown in the scheme. Resorcinol was obtained commercially and used without further purification. 4-Benzyloxybenzoic acid, 2-fluoro-4-benzyloxybenzoic acid and 3-fluoro-4-benzyloxybenzoic acids were prepared according to the procedure we described elsewhere [23]. 2-Fluoro-4-*n*-alkoxybenzoic acids and 3-fluoro-4-*n*-alkoxybenzoic acids were synthesized by a procedure described in the literature [24]. The detailed procedure for the synthesis and characterization of one of the compounds under investigation is given below.

2.1.1. 1,3-Phenylene bis(2-fluoro-4-benzyloxybenzoate), *c* ($R_1 = F$, $R_2 = H$)

A mixture of 1,3-dihydroxybenzene, **a** (1.1 g, 10 mmol), 2-fluoro-4-benzyloxybenzoic acid, **b** (4.92 g, 20 mmol), a catalytic amount of 4-(*N,N*-dimethylamino)pyridine (DMAP) and dry dichloromethane (25 ml) was stirred for about 10 min at room temperature. To this mixture, *N,N*-dicyclohexylcarbodiimide (DCC) (4.9 g, 24 mmol) was added and stirring continued for about 8–10 h at room temperature. The precipitated *N,N*-dicyclohexylurea was filtered off and washed with



Scheme. General synthetic pathway used for the preparation of banana-shaped mesogens.

excess of dichloromethane (75 ml). The filtered solution was washed with 5% aqueous acetic acid (2 × 50 ml), 5% cold aqueous sodium hydroxide (2 × 50 ml) and finally with water (3 × 50 ml) and dried over anhydrous sodium sulphate. The crude residue obtained after removal of solvent was chromatographed on silica gel using chloroform as eluent. Removal of solvent from the eluate afforded a white material which was recrystallized from acetonitrile; yield 4.6 g (82%), m.p. 161–162°C. ¹H NMR (CDCl₃, 400 MHz) δ(ppm): 8.05 (t, 2H, Ar-H, *J*=8.6 Hz), 7.46–7.36 (m, 11H, Ar-H), 7.17–7.13 (m, 3H, Ar-H), 6.85 (dd, 2H, Ar-H, ³*J*=8.9 Hz, ⁴*J*=2.4 Hz), 6.76 (dd, 2H, Ar-H, ³*J*=12.5 Hz, ⁴*J*=2.4 Hz), 5.14 (s, 4H, 2 × ArCH₂O-). IR (KBr) ν_{max}: 3050, 2931, 1728, 1620, 1598, 1575, 1504, 1431, 1342, 1253, 1130 cm⁻¹.

2.1.2. *1,3-Phenylene bis(2-fluoro-4-hydroxybenzoate)*,
d (*R*₁=*F*, *R*₂=*H*)

To a solution of compound **c** (4.0 g) in 1,4-dioxane (50 ml), 5% Pd-C catalyst (0.8 g) was added. The mixture was stirred at 50°C in an atmosphere of hydrogen till the calculated quantity of hydrogen was absorbed. The resultant mixture was filtered hot and the solvent removed under reduced pressure. The residue obtained was passed through a column of silica gel and eluted with a mixture of 5% acetone in chloroform. The eluate gave a white material which was recrystallized from a mixture of butan-2-one and petroleum-ether (b.p. 60–80°C); yield 2.4 g (88%), m.p. 270–272°C. ¹H NMR (CDCl₃, 400 MHz) δ(ppm): 9.97 (s, 2H, 2 × Ar-OH), 8.15 (t, 2H, Ar-H, *J*=8.7 Hz), 7.67 (t, 1H, Ar-H, *J*=8.3 Hz), 7.37–7.33 (m, 3H, Ar-H), 6.97 (dd, 2H, Ar-H, ³*J*=8.8 Hz, ⁴*J*=2.3 Hz), 6.87 (dd, 2H, ³*J*=12.8 Hz, ⁴*J*=2.3 Hz). IR (KBr) ν_{max}: 3331, 3065, 2962, 1726, 1712, 1600, 1504, 1452, 1211, 1124 cm⁻¹.

2.1.3. *1,3-Phenylene bis[4-(2-fluoro-4-*n*-undecyloxybenzyoyloxy)-2-fluorobenzoate]*,
e (*R*₁=*F*, *R*₂=*H*, *R*₃=*F*, *R*₄=*H*, *n*=11)

Compound **d** (0.25 g, 0.65 mmol) and 2-fluoro-4-*n*-undecyloxybenzoic acid (0.4 g, 1.3 mmol) were dissolved in dry dichloromethane (10 ml) and a catalytic quantity of DMAP added to it and the resultant reaction mixture was stirred for about 10 min. DCC (0.32 g, 1.5 mmol) was added and the stirring continued for 8–10 h; the precipitated *N,N'*-dicyclohexylurea was filtered off and washed with chloroform (30 ml). Removal of solvent afforded a crude material which was passed through a column of silica gel using toluene as eluent. The white material obtained after removal of solvent from the eluate was recrystallized from a mixture of chloroform and ethyl alcohol; yield 0.41 g

(60%), m.p. 78°C. ¹H NMR (CDCl₃, 400 MHz) δ(ppm): 8.2–8.16 (m, 2H, Ar-H), 8.04 (t, 2H, Ar-H, *J*=8.6 Hz), 7.5 (t, 1H, Ar-H, *J*=8.4 Hz), 7.23–7.17 (m, 7H, Ar-H), 6.79 (dd, 2H, Ar-H, ³*J*=8.9 Hz, ⁴*J*=2.4 Hz), 6.70 (dd, 2H, Ar-H, ³*J*=12.8 Hz, ⁴*J*=2.3 Hz), 4.03 (t, 4H, 2 × Ar-O-CH₂, *J*=6.5 Hz), 1.82 (quin, 4H, 2 × Ar-OCH₂-CH₂, *J*=7.9 Hz), 1.46 (quin, 4H, 2 × Ar-O-CH₂-CH₂-CH₂, *J*=7.8 Hz), 1.4–1.2 (m, 28H, 14 × -CH₂-), 0.88 (t, 6H, 2 × -CH₃, *J*=6.7 Hz). ¹³C NMR (CDCl₃, 400 MHz) δ(ppm): 165.5, 165.4, 164.2, 162.9, 161.7, 161.6, 161.4, 155.9, 155.8, 151.1, 133.9, 133.5, 129.9, 119.5, 117.9, 115.8, 115.2, 111.6, 111.3, 111.1, 108.9, 103.2, 102.9, 69.0, 31.9, 29.6, 29.5, 29.3, 28.9, 25.9, 22.7, 14.1. IR (KBr) ν_{max}: 3066, 2924, 2852, 1755, 1743, 1730, 1620, 1576, 1506, 1477, 1434, 1176 cm⁻¹.

2.2. Characterization

The intermediates and the target compounds were purified by column chromatography on silica gel, (ACME make, 60–120 mesh) using suitable solvents for elution. All the compounds were crystallized using appropriate solvents to constant melting points. Merck Kieselgel 60F₂₅₄ precoated thin layer chromatographic plates were used to check the purity of all the compounds by exposing the plates to a UV lamp at 254 nm. The normal phase high performance liquid chromatography on a μ-porasil column, (3.9 mm × 300 mm, Waters Associates Inc.) was used to determine the purity of all the target compounds using 1% ethyl acetate in dichloromethane as eluent. The yield obtained for all the intermediate compounds was in the range 70–90%, while for the final compounds it was about 50–75%. ¹H NMR spectra were used to confirm the chemical structure of intermediates as well as the target compounds; ¹³C NMR spectra were recorded only for the target compounds using 1% tetramethylsilane in deuteriochloroform as an internal standard on a Bruker AMX 400 spectrometer. Infrared absorption spectra were recorded on a Shimadzu FTIR-8400 spectrophotometer using a KBr disk, and the elemental analysis was carried out on a Carlo-Erba 1106 analyser.

The mesophase behaviour of all the target compounds was examined under a Leitz Laborlux 12 POL/Olympus BX 50 polarizing optical microscope equipped with a FP5 heating stage and a FP52 controller, by sandwiching the sample between a glass slide and a coverslip. The transition temperatures and the associated enthalpies were calculated from thermograms recorded on a Perkin-Elmer, Model Pyris 1D differential scanning calorimeter. The calorimeter was calibrated using pure indium as a standard. The X-ray diffraction (XRD) studies of the unoriented samples were carried out using CuK_α radiation (λ=1.54 Å)

from a rotating anode generator, Rigaku Ultrax 18 with a flat graphite crystal monochromator. Samples were taken in Lindemann capillaries of 0.7 mm diameter and the diffraction patterns of the samples were collected on an image plate (Marresearch) while the sample temperature was controlled to within $\pm 0.5^\circ\text{C}$. In order to confirm whether the mesophases are ferro-/antiferro-electric in nature and to determine the value of spontaneous polarization, the triangular wave method was employed. The samples were taken in polyimide-coated ITO cells and triangular wave, modified triangular waves were generated using an Arbitrary Waveform Generator (Wavetek, Model 395), which was amplified using a Trek Model 601B-3 amplifier. The current was measured across a 10 k Ω series resistor and the current response traces were recorded using a Tektronix Oscilloscope, TDS220. The electro-optical switching characteristics were examined using a simple experimental set-up where the polyimide-coated ITO cells with samples were heated on the hot stage of a polarizing microscope and the d.c. field applied using a Regulated Dual d.c. Power Supply. The switching characteristics were observed under the microscope.

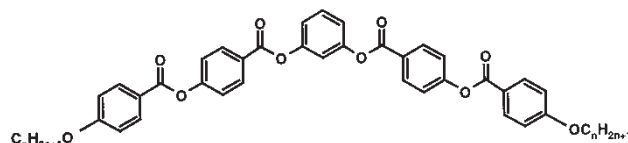
3. Results and discussion

3.1. Mesomorphic properties

A total of 101 compounds composed of banana-shaped molecules belonging to 11 different homologous series have been investigated. This systematic study has been carried out to examine the influence of a fluorine substituent on the mesomorphic behaviour of five-ring esters. In any such study, the starting point would be to examine the liquid crystalline properties of the unsubstituted parent compounds (series I). The transition temperatures and associated enthalpies of the compounds of this series are summarized in table 1. As reported [25] earlier, all 15 homologues are mesomorphic and B_6 , B_1 and B_2 phases have been observed. Interestingly, the shortest homologue (compound 1) shows the banana phase (B_6) and is monotropic. The methoxy group of this compound can be considered as part of the core which stabilizes the intercalated structure, which perhaps is due to the opposing dipoles. On increasing the chain length, the core-core interactions are reduced by the electropositive alkyl chains and hence the B_6 phase is stabilized. It is also appropriate to note here that compound 8 has been reported [1] to exhibit an enantiotropic B_1 phase with a melting point of 111°C . However, we observe only a monotropic B_1 phase. For compound 10, the B_1 phase is observed on cooling only over a very narrow temperature range of 1°C in addition to a B_2 phase [26]. The transition temperatures of compounds 12 and 13 agree fairly well with the literature [26]. A plot of the transition

Table 1. Transition temperatures ($^\circ\text{C}$) and associated enthalpy changes (kJ mol^{-1}) (*in italics*) for series I [25].

Key: Cr = crystalline phase; B_1 = two-dimensional banana phase; B_2 = lamellar antiferroelectric banana phase; B_6 = intercalated smectic banana phase; B_{X1} = banana ferroelectric lamellar phase; B_{X2} = banana ferroelectric two-dimensional phase; I = isotropic phase; temperature in parentheses indicates monotropic transition.



| Compound | <i>n</i> | Cr | B_2 | B_1 | B_6 | I |
|----------|----------|------------------------|--------------------------|--------------------------|--------------------------|---|
| 1 | 1 | • 168.5 <i>46.3</i> | — | — | (• 143.5) <i>9.3</i> | • |
| 2 | 2 | • 173.0 <i>49.3</i> | — | — | (• 167.5) <i>11.6</i> | • |
| 3 | 3 | • 175.0 <i>53.2</i> | — | — | (• 160.5) <i>12.9</i> | • |
| 4 | 4 | • 157.5 <i>37.6</i> | — | — | • 161.5 <i>14.9</i> | • |
| 5 | 5 | • 170.0 <i>82.0</i> | — | — | (• 148.5) <i>15.5</i> | • |
| 6 | 6 | • 138.5 <i>48.9</i> | — | • 140.5 <i>17.8</i> | — | • |
| 7 | 7 | • 132.5 <i>54.4</i> | — | (• 129.5) <i>17.7</i> | — | • |
| 8 | 8 | • 124.5 <i>66.2</i> | — | (• 123.0) <i>19.1</i> | — | • |
| 9 | 9 | • 115.0 <i>75.1</i> | — | (• 114.0) <i>18.3</i> | — | • |
| 10 | 10 | • 111.5 <i>54.6</i> | (• 110.0) <i>20.3</i> | — | — | • |
| 11 | 11 | • 105.0 <i>38.3</i> | • 113.5 <i>21.6</i> | — | — | • |
| 12 | 12 | • 106.0 <i>42.7</i> | • 116.5 <i>22.5</i> | — | — | • |
| 13 | 14 | • 107.0 <i>50.6</i> | • 119.5 <i>24.3</i> | — | — | • |
| 14 | 16 | • 110.5 <i>81.8</i> | • 121.5 <i>25.6</i> | — | — | • |
| 15 | 18 | • 112.0 <i>68.9</i> | • 121.5 <i>24.5</i> | — | — | • |

temperatures as a function of the number of carbon atoms in the terminal *n*-alkoxy chains for series I is shown in figure 2. It can be seen that the B_1 -I and B_2 -I transition temperatures follow the general trends observed previously [23].

In the case of series II, a fluorine substituent (R_1) is introduced *ortho* to the carbonyl ester group connected to the central phenyl ring. The transition temperatures together with the associated enthalpy changes of this series are given in table 2. It can be seen that the mesomorphic behaviour of the homologues of this series is similar to that observed for compounds of

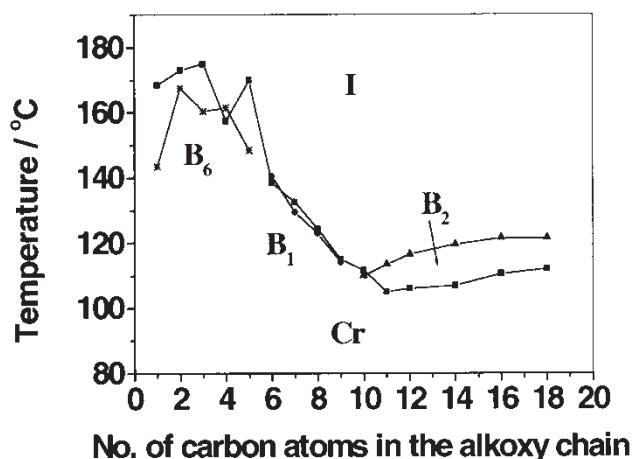


Figure 2. A plot of transition temperature as a function of terminal chain length for series I.

series I. While there is a general decrease in the melting as well as the clearing temperatures, the metastable phases become enantiotropic as a result of this fluorine substitution. However, a monotropic B_1 phase observed for compound **9** is totally eliminated as a result of this substitution (compound **24**). Apart from the core and the lateral substituents, the length of the terminal alkyl chains also play an important role with regard to the stability of the individual mesophases. As can be seen in series I and II, the B_6 phase occurs as a metastable phase, becomes enantiotropic on ascending the series and becomes monotropic again after a certain chain length (for example compounds **1–5** and **16–20**). One can see that for compound **20** the melting point is rather high, as a result of which a metastable phase is seen. On further increasing the chain length, the core–core and the tail–tail interactions increase and hence the molecules exist as clusters. These arrange in a two-dimensional rectangular fashion such that the polarization due to the clusters is reduced, which helps in the further stabilization of the intercalated structure. As usual, the compounds of longer chains exist in smectic layers. A plot of transition temperature as a function of the number of carbon atoms in the terminal n -alkoxy chains for series II is shown in figure 3.

When a fluorine substituent is in the *meta*-position (R_2) as in series III, the mesogenic properties are completely suppressed and only one compound (**32**) exhibits a monotropic B_6 phase. In table 3, the melting points and associated enthalpy changes, the clearing temperature and the associated enthalpy change for compound **32** are given. It is interesting to note that the melting points of these compounds are higher than those of the corresponding members of series II. This suggests that dipolar effects play a more important role than steric

Table 2. Transition temperatures ($^{\circ}\text{C}$) and associated enthalpy changes (kJ mol^{-1}) (*in italics*) for series II [25]. For key see table 1.

| Compound | n | Cr | B_2 | B_1 | B_6 | I |
|----------|-----|------------------------|------------------------|--------------------------|--------------------------|---|
| 16 | 1 | • 176.0 <i>63.0</i> | — | — | (• 125.5) ^a | • |
| 17 | 2 | • 152.0 <i>42.9</i> | — | — | • 155.0 <i>10.8</i> | • |
| 18 | 3 | • 126.5 <i>26.6</i> | — | — | • 147.0 <i>11.9</i> | • |
| 19 | 4 | • 128.5 <i>40.4</i> | — | — | • 146.0 <i>13.3</i> | • |
| 20 | 5 | • 139.0 <i>64.1</i> | — | — | (• 130.0) <i>11.6</i> | • |
| 21 | 6 | • 108.0 <i>29.0</i> | — | • 121.5 <i>15.8</i> | — | • |
| 22 | 7 | • 118.5 <i>57.1</i> | — | (• 109.5) <i>15.2</i> | — | • |
| 23 | 8 | • 112.0 <i>58.7</i> | — | (• 101.0) <i>15.8</i> | — | • |
| 24 | 9 | • 97.0 <i>65.2</i> | — | — | — | • |
| 25 | 10 | • 96.5 <i>44.9</i> | • 98.0 <i>19.8</i> | — | — | • |
| 26 | 11 | • 95.0 <i>49.4</i> | • 101.0 <i>20.8</i> | — | — | • |
| 27 | 12 | • 93.0 <i>48.1</i> | • 105.0 <i>22.8</i> | — | — | • |
| 28 | 14 | • 91.0 <i>44.4</i> | • 109.0 <i>21.9</i> | — | — | • |
| 29 | 16 | • 94.5 <i>63.2</i> | • 110.5 <i>24.4</i> | — | — | • |
| 30 | 18 | • 99.5 <i>87.9</i> | • 112.5 <i>26.0</i> | — | — | • |

^aEnthalpy could not be determined as the sample crystallizes immediately.

factors in determining the formation of mesophases by these five-ring esters.

Now let us turn attention to the terminal phenyl ring. When a fluorine substituent is introduced on the terminal phenyl ring ($R_3 = \text{F}$, series IV), the occurrence of mesophases is similar to that observed for series II. In other words, the intercalated mesophase B_6 , the two-dimensional rectangular columnar mesophase B_1 and the antiferroelectric mesophase B_2 are obtained on ascending the series. The homologue at which the crossover from the B_1 to B_2 phase takes place on ascending the series, namely compound **47**, exhibits a highly metastable B_2 phase on rapid cooling and neither the temperature nor the associated enthalpy change could be determined using DSC. The transition temperatures

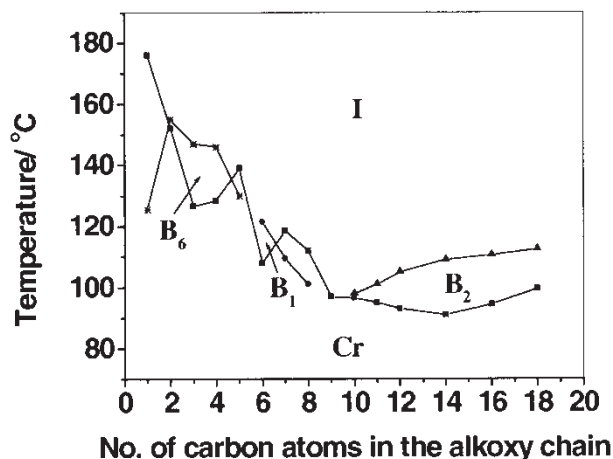


Figure 3. A plot of transition temperature as a function of terminal chain length for series II.

together with the associated enthalpy changes for series IV are collected in table 4. From this table it is clear that the two-dimensional B_1 phase is suppressed more, when compared with the intercalated B_6 phase, as a result of the substitution. All the compounds that exhibit a B_6 phase show the same type of texture when the isotropic liquid is cooled slowly. A typical photomicrograph of the texture of the B_6 mesophase of compound 43 is

Table 3. Transition temperatures ($^{\circ}\text{C}$) and associated enthalpy changes (kJ mol^{-1}) (*in italics*) for series III [25]. For key see table 1.

| Compound | n | Cr | B_6 | I |
|----------|-----|--------------------------------------|-------------------------|---|
| 31 | 3 | ● 137.0 <i>48.0</i> | — | ● |
| 32 | 4 | ● 130.0 <i>50.5</i> | (● 109.0) <i>9.4</i> | ● |
| 33 | 5 | ● 142.0 <i>61.3</i> | — | ● |
| 34 | 6 | ● 124.5 <i>50.2</i> | — | ● |
| 35 | 7 | ● 125.5 <i>57.7</i> | — | ● |
| 36 | 8 | ● 125.0 <i>52.2</i> | — | ● |
| 37 | 9 | ● 125.5 <i>56.4</i> | — | ● |
| 38 | 14 | ● 122.5 ^a <i>97.4</i> | — | ● |
| 39 | 18 | ● 120.0 ^a <i>113.5</i> | — | ● |

^aCompound has crystal-crystal transition; enthalpy denoted is the sum of all previous transitions.

Table 4. Transition temperatures ($^{\circ}\text{C}$) and associated enthalpy changes (kJ mol^{-1}) (*in italics*) for series IV. For key see table 1.

| Compound | n | Cr | B_2 | B_1 | B_6 | I |
|-----------------|-----|------------------------|-------------------------|--------------------------|--------------------------|---|
| 40 | 3 | ● 151.0 <i>48.0</i> | — | — | — | ● |
| 41 | 4 | ● 133.5 <i>38.6</i> | — | — | (● 129.0) <i>11.1</i> | ● |
| 42 | 5 | ● 148.0 <i>64.7</i> | — | — | (● 123.5) <i>12.0</i> | ● |
| 43 | 6 | ● 117.0 <i>34.3</i> | — | — | ● 120.0 <i>13.3</i> | ● |
| 44 | 7 | ● 112.0 <i>46.0</i> | — | (● 111.0) <i>15.4</i> | — | ● |
| 45 | 8 | ● 107.0 <i>64.5</i> | — | (● 105.0) <i>15.9</i> | — | ● |
| 46 | 9 | ● 103.5 <i>80.1</i> | — | (● 95.0) ^a | — | ● |
| 47 ^b | 10 | ● 106.5 <i>55.6</i> | — | — | — | ● |
| 48 | 11 | ● 101.0 <i>68.7</i> | (● 97.0) <i>19.9</i> | — | — | ● |
| 49 | 12 | ● 100.0 <i>38.5</i> | ● 101.0 <i>21.2</i> | — | — | ● |
| 50 | 14 | ● 99.0 <i>63.2</i> | ● 106.0 <i>23.0</i> | — | — | ● |
| 51 | 16 | ● 91.0 <i>67.3</i> | ● 108.5 <i>24.8</i> | — | — | ● |
| 52 | 18 | ● 95.0 <i>75.4</i> | ● 110.0 <i>25.4</i> | — | — | ● |

^aEnthalpy could not be determined as the sample crystallizes immediately.

^bOn fast cooling of the isotropic liquid under a polarizing microscope, B_2 phase appears and crystallizes immediately; neither the exact temperature nor the enthalpy could be determined.

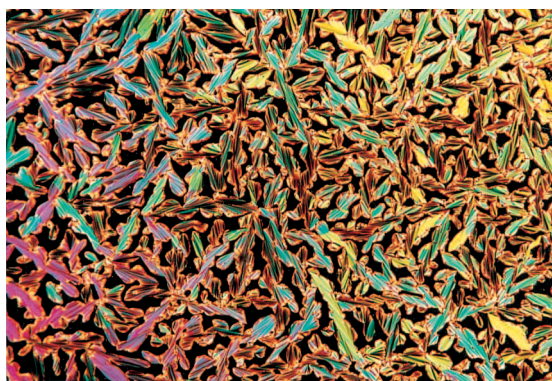


Figure 4. Optical photomicrograph of a fan-shaped texture obtained for the B_6 mesophase of compound 43 on cooling the isotropic liquid.

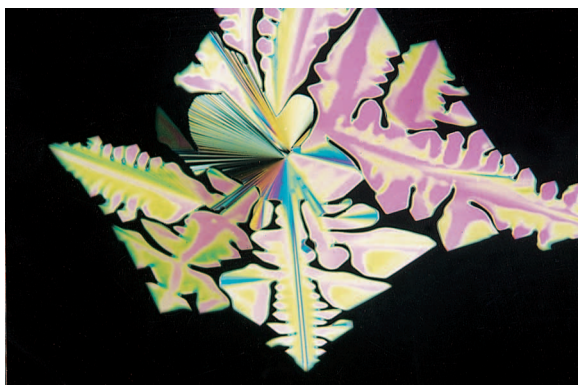


Figure 5. Optical photomicrograph of the growth of spherulitic and dendritic patterns obtained for the B_1 mesophase of compound **44** on cooling the isotropic liquid.

shown in figure 4. However, the two-dimensional B_1 phase shows both spherulites and dendritic patterns as it grows from the isotropic phase. An optical photomicrograph of the growth of the B_1 mesophase of compound **44** is shown in figure 5. The textures exhibited by the well studied lamellar antiferroelectric B_2 phase has been reported by a number of researchers [12, 19, 26, 27]. A typical photomicrograph of the mesophase of compound **50** is shown in figure 6. A plot of the transition temperatures as a function of the number of carbon atoms in the terminal chains is shown in figure 7. The clearing temperature curves for these three phases are typical for such transitions as observed in a number of other series of compounds.

However, when a fluorine is substituted *ortho* to the terminal *n*-alkoxy chain ($R_4 = F$) very interesting phase behaviour is observed (series V). The transition temperatures and the associated enthalpy changes for series V are summarized in table 5. For compounds with chains containing less than or equal to 11 carbon atoms no mesophase is observed, which is in contrast to what is

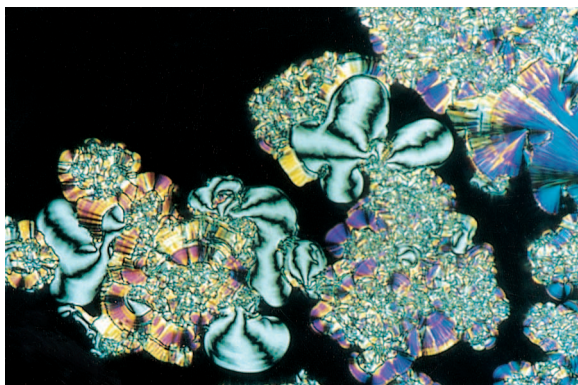


Figure 6. Optical photomicrograph of the schlieren and other patterns obtained for the B_2 mesophase of compound **50** on cooling the isotropic liquid.

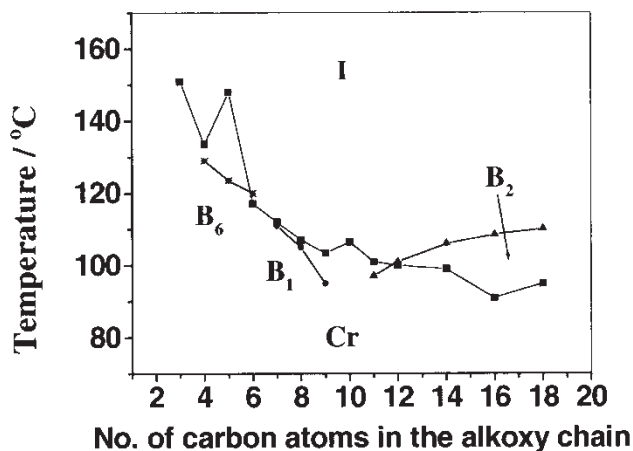
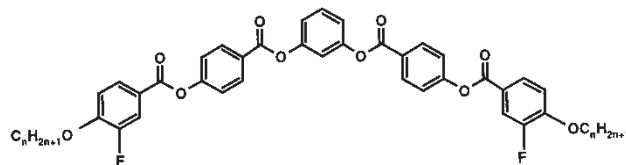


Figure 7. A plot of transition temperature as a function of terminal chain length for series IV.

observed for homologues of series IV. In other words, the intercalated B-phases namely, B_6 and B_1 , are completely suppressed. Even more interestingly, as we recently reported [21], compounds **57** to **59** show a lamellar phase with a grainy texture on heating. However, on cooling the mesophase appears dark and by

Table 5. Transition temperatures ($^{\circ}\text{C}$) and associated enthalpy changes (kJ mol^{-1}) (*in italics*) for series V [21]. For key see table 1.



| Compound | <i>n</i> | Cr | B_{X2} | B_{X1} | I |
|-----------|----------|----------------------|-------------|-------------|---|
| 53 | 7 | • 130.0 ^a | — | — | • |
| | | <i>73.3</i> | | | |
| 54 | 9 | • 130.0 | — | — | • |
| | | <i>47.6</i> | | | |
| 55 | 10 | • 129.0 ^a | — | — | • |
| | | <i>85.7</i> | | | |
| 56 | 11 | • 129.0 ^a | — | — | • |
| | | <i>111.0</i> | | | |
| 57 | 12 | • 128.0 ^a | — | (• 127.5) | • |
| | | <i>110.0</i> | | <i>21.8</i> | |
| | | | | | |
| 58 | 14 | • 124.0 ^a | — | • 128.5 | • |
| | | <i>97.9</i> | | <i>23.3</i> | |
| 59 | 16 | • 121.0 ^a | — | • 129.0 | • |
| | | <i>104.9</i> | | <i>24.3</i> | |
| | | | | | |
| 60 | 18 | • 118.0 ^a | • 128.5 | — | • |
| | | <i>125.7</i> | <i>24.4</i> | | |
| | | | | | |
| 61 | 20 | • 117.5 ^a | • 127.0 | — | • |
| | | <i>95.8</i> | <i>24.5</i> | | |

^aCompound has crystal-crystal transition; enthalpy denoted is the sum of all previous transitions.



Figure 8. A complex textural pattern obtained for the B_{X2} mesophase of compound **61** on cooling the isotropic liquid.

rotating the polarizer or analyzer domains of opposite handedness are observed and the mesophase exhibits ferroelectric properties. The mesophase of compounds **60** and **61** shows a two-dimensional pattern as determined by XRD. This mesophase is less viscous although not lamellar, and shows ferroelectric properties. A typical texture of this B_{X2} phase obtained on cooling the isotropic liquid of compound **61** is shown in figure 8. As reported recently [21] this type of behaviour represents the first example of two different mesophases exhibited by homologues of the same series which show ferroelectric properties.

In both these phases, namely B_{X1} ($SmC_S P_F$) and B_{X2} (structure not yet determined), the melting as well as the clearing temperatures are drastically increased when compared with either the parent series I or any of the other fluorine-substituted mesogens in these five-ring esters. This is due perhaps to the fluorine in the *ortho*-position influencing a change in the conformation of either the core or the terminal chains, such that the

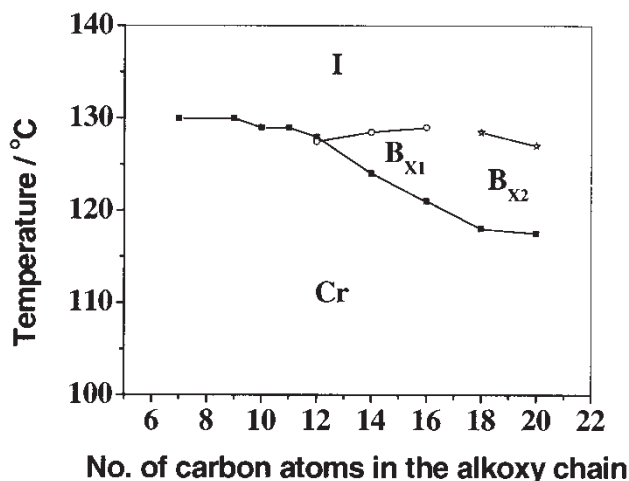
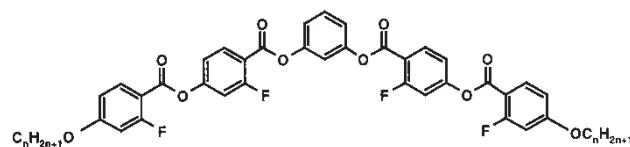


Figure 9. A plot of transition temperature as a function of terminal chain length for series V.

packing efficiency increases. It is appropriate to mention here that Bedel *et al.* [18, 19] have also observed ferroelectric properties in five-ring Schiff's base esters in which a fluorine is substituted *ortho* to the terminal *n*-alkoxy chain. A plot of the transition temperature as a function of the number of carbon atoms in the terminal *n*-alkoxy chains for series V is shown in figure 9.

Now let us examine the mesomorphic behaviour of compounds which contain a fluorine substituent in each of the phenyl rings on the arms of these bent-core materials. The transition temperatures and the associated enthalpy changes for fifteen compounds of series VI are summarized in table 6. In this series the fluorine

Table 6. Transition temperatures ($^{\circ}C$) and associated enthalpy changes ($kJ\ mol^{-1}$) (*in italics*) for series VI. For key see table 1.



| Compound | <i>n</i> | Cr | B_2 | B_1 | B_6 | I |
|-----------------------|----------|------------------------|--------------------------------------|-----------|-----------|---|
| 62 | 1 | ● 161.5 <i>59.4</i> | — | — | — | ● |
| 63^a | 2 | ● 162.5 <i>59.2</i> | — | — | — | ● |
| 64 | 3 | ● 132.0 <i>48.2</i> | — | — | (● 120.0) | ● |
| 65 | 4 | ● 130.5 <i>52.2</i> | — | — | (● 127.5) | ● |
| 66 | 5 | ● 129.0 <i>64.9</i> | — | — | (● 115.5) | ● |
| 67 | 6 | ● 109.0 <i>48.0</i> | — | (● 108.0) | — | ● |
| 68 | 7 | ● 100.0 <i>46.5</i> | — | (● 96.0) | — | ● |
| 69 | 8 | ● 95.5 <i>48.8</i> | — | (● 87.5) | — | ● |
| 70^b | 9 | ● 94.0 <i>52.1</i> | — | — | — | ● |
| 71 | 10 | ● 96.0 <i>58.0</i> | (● 81.5) ^c <i>18.7</i> | — | — | ● |
| 72 | 11 | ● 78.0 <i>23.9</i> | ● 87.5 | — | — | ● |
| 73 | 12 | ● 97.0 <i>58.4</i> | (● 92.0) | — | — | ● |
| 74 | 14 | ● 87.0 <i>69.1</i> | ● 97.5 | — | — | ● |
| 75 | 16 | ● 93.5 <i>81.8</i> | ● 101.0 | — | — | ● |
| 76 | 18 | ● 97.0 <i>93.8</i> | ● 102.5 | — | — | ● |

^aOn fast cooling of the isotropic liquid under a polarizing microscope, B_6 phase appears and crystallizes immediately.

^bOn fast cooling of the isotropic liquid under a polarizing microscope, B_1 phase appears and crystallizes immediately.

^cTemperature obtained during cooling cycle.

is substituted *ortho* to the two carbonyl groups. As compared with the unsubstituted compounds (series I), there is a general decrease of the melting points for all the homologues. More importantly, although the three mesophases B_2 , B_1 and B_6 are retained in the series, they are suppressed to a large extent. For example, compound **62** is non-mesomorphic while compound **63** shows a highly metastable B_6 phase. Since the mesophase crystallizes immediately, it has not been possible to determine the temperature or associated enthalpy change for this transition. Compounds **64–69**, **71** and **73** are all monotropic and only four are enantiotropic. Compound **70** displays a highly metastable columnar B_1 phase on fast cooling of the isotropic liquid under a polarizing microscope and sometimes crystallizes directly. In contrast, 14 of the monofluoro-substituted compounds (series II) are mesomorphic. A plot of the transition temperature as a function of the length of the *n*-alkoxy chain for this series is shown in figure 10. The general trends observed for other series of compounds are also seen here.

In the case of compounds of series VII, there is a fluorine substituted *ortho* to the terminal *n*-alkoxy chain and a fluorine *ortho* to the carbonyl group. It is interesting to note that the antiferroelectric B_2 phase is replaced by a lamellar phase which shows ferroelectric properties. Compounds **77** and **78** show a monotropic B_6 phase while compounds **79** and **80** exhibit a monotropic B_1 phase and compound **81** is non-mesomorphic; compounds **82–89** are all enantiotropic. A plot of the transition temperature as a function of the length of the *n*-alkoxy chain is shown in figure 11.

As in the previous case, there is a general reduction in the melting as well as clearing points of series VII

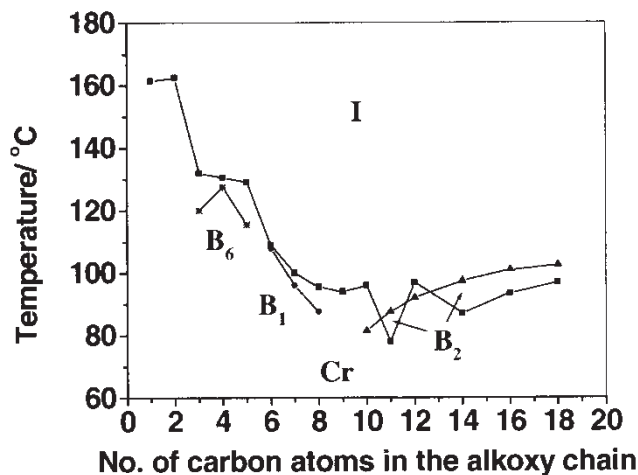


Figure 10. A plot of transition temperature as a function of terminal chain length for series VI.

Table 7. Transition temperatures ($^{\circ}\text{C}$) and associated enthalpy changes (kJ mol^{-1}) (*in italics*) for series VII. For key see table 1.

| Compound | <i>n</i> | Cr | B_{X1} | B_1 | B_6 | I |
|----------|----------|----------------------|-------------|-----------|-------------|---|
| 77 | 4 | • 144.0 | — | — | (• 141.0) | • |
| | | <i>53.7</i> | | | <i>14.3</i> | |
| 78 | 5 | • 149.0 | — | — | (• 128.0) | • |
| | | <i>74.9</i> | | | <i>14.5</i> | |
| 79 | 6 | • 129.0 | — | (• 117.5) | — | • |
| | | <i>56.2</i> | | | <i>15.5</i> | |
| 80 | 7 | • 107.5 | — | (• 106.0) | — | • |
| | | <i>79.2</i> | | | <i>15.3</i> | |
| 81 | 8 | • 108.0 | — | — | — | • |
| | | <i>78.8</i> | | | | |
| 82 | 9 | • 107.0 | • 110.5 | — | — | • |
| | | <i>74.8</i> | <i>19.7</i> | | | |
| 83 | 10 | • 105.0 | • 113.5 | — | — | • |
| | | <i>57.1</i> | <i>21.6</i> | | | |
| 84 | 11 | • 106.0 ^a | • 115.5 | — | — | • |
| | | <i>92.4</i> | <i>22.1</i> | | | |
| 85 | 12 | • 99.5 ^a | • 117.5 | — | — | • |
| | | <i>92.8</i> | <i>23.1</i> | | | |
| 86 | 14 | • 103.0 ^a | • 120.5 | — | — | • |
| | | <i>104.5</i> | <i>24.2</i> | | | |
| 87 | 16 | • 105.0 ^a | • 122.0 | — | — | • |
| | | <i>109.6</i> | <i>24.6</i> | | | |
| 88 | 18 | • 107.0 ^a | • 122.0 | — | — | • |
| | | <i>131.7</i> | <i>25.2</i> | | | |
| 89 | 20 | • 108.0 ^a | • 121.0 | — | — | • |
| | | <i>120.9</i> | <i>26.0</i> | | | |

^aCompound has crystal–crystal transition; enthalpy denoted is the sum of all previous transitions.

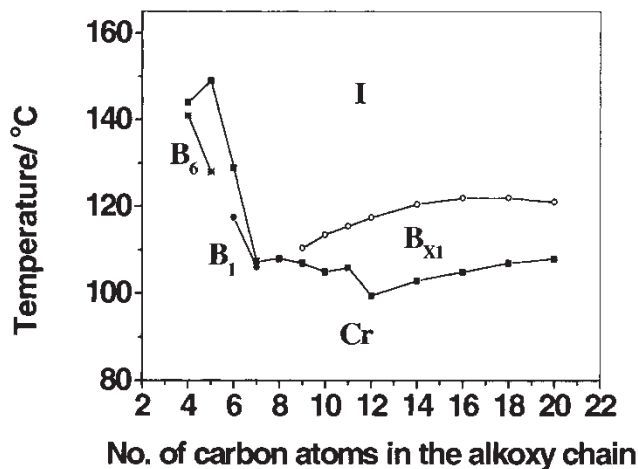
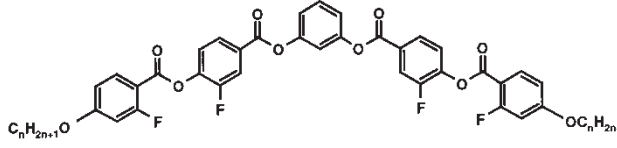


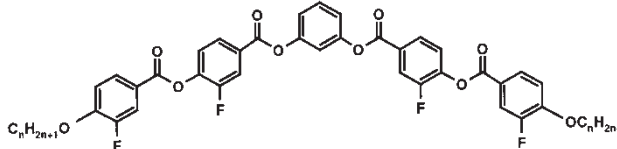
Figure 11. A plot of transition temperature as a function of terminal chain length for series VII.

Table 8. Transition temperatures ($^{\circ}\text{C}$) and associated enthalpy changes (kJ mol^{-1}) (*in italics*) for series VIII. For key see table 1.



| Compound | n | Cr | I | |
|----------|-----|----|-------------|---|
| 90 | 6 | ● | 114.0 | ● |
| | | | <i>43.8</i> | |
| 91 | 14 | ● | 113.0 | ● |
| | | | <i>67.8</i> | |

Table 9. Transition temperatures ($^{\circ}\text{C}$) and associated enthalpy changes (kJ mol^{-1}) (*in italics*) for series IX. For key see table 1.

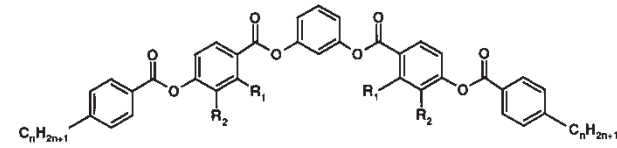


| Compound | n | Cr | I | |
|----------|-----|----|-------------|---|
| 92 | 6 | ● | 160.0 | ● |
| | | | <i>63.1</i> | |
| 93 | 14 | ● | 152.0 | ● |
| | | | <i>84.9</i> | |

when compared with those of the unsubstituted compounds (series I). It is remarkable to note that two fluoro substituents enhance the mesogenic character of these compounds. For example, compounds **53–56** which are monofluoro-substituted derivatives are non-mesomorphic while the corresponding difluoro-substituted compounds **80**, **82** to **84** are all mesomorphic. In addition, compounds **82–89** show a lamellar mesophase (B_{X1}) with ferroelectric characteristics as mentioned earlier (compounds **57–59**). The two-dimensional ferroelectric phase obtained for compounds **60** and **61** is not observed in this series.

The position of fluorine substitution is really very critical for the formation of the mesophase. If a fluorine is substituted *meta* to the carbonyl group of the first phenyl moiety, then irrespective of the position of the fluorine substituent on the terminal phenyl group of these five-ring esters, no mesophase is observed. This behaviour is illustrated with two derivatives of each of the series VIII and IX respectively (compounds **90–93**) and the latter show very high melting points. This in itself is strong proof for the dipolar effects in

Table 10. Transition temperatures ($^{\circ}\text{C}$) and associated enthalpy changes (kJ mol^{-1}) (*in italics*) for series X and XI [25]. For key see table 1.



| Compound | R_1 | R_2 | n | Cr | B_2 | I | | |
|----------|-------|-------|-----|----|--------------|---|-------|---|
| 94 | F | H | 8 | ● | 100.5 | — | ● | |
| | | | | | <i>49.6</i> | | | |
| 95 | F | H | 9 | ● | 104.5 | — | ● | |
| | | | | | <i>53.3</i> | | | |
| 96 | F | H | 10 | ● | 102.5 | — | ● | |
| | | | | | <i>49.2</i> | | | |
| 97 | F | H | 11 | ● | 101.5 | ● | 104.0 | ● |
| | | | | | <i>28.5</i> | ● | 22.2 | |
| 98 | F | H | 12 | ● | 99.5 | ● | 105.5 | ● |
| | | | | | <i>31.2</i> | ● | 23.9 | |
| 99 | F | H | 14 | ● | 97.5 | ● | 108.5 | ● |
| | | | | | <i>55.1</i> | ● | 25.9 | |
| 100 | F | H | 16 | ● | 96.5 | ● | 110.5 | ● |
| | | | | | <i>42.5</i> | ● | 26.6 | |
| 101 | H | F | 14 | ● | 97.0 | — | — | ● |
| | | | | | <i>100.2</i> | | | |

such compounds playing an important role in inducing mesophase/s.

In order to study the effect of a terminal *n*-alkyl chain as opposed to an *n*-alkoxy chain, we examined only two series of compounds. For example, in series X there is a fluorine substituent *ortho* to the carbonyl group of the first phenyl moiety and an *n*-alkyl chain. The transition temperatures and the associated enthalpy changes for this series are summarized in table 10. As can be seen, only one mesophase type was observed and the antiferroelectric B_2 phase was obtained for chain lengths where $n \geq 11$ and all are enantiotropic. The thermal range of the mesophase appears to be reduced when there is a terminal *n*-alkyl group. While comparing the *n*-alkoxy and *n*-alkyl chains (series II and X), the *n*-alkoxy terminal chains stabilize the intercalated B_6 and B_1 phases in addition to the antiferroelectric B_2 phase. We made only one derivative (compound **101**) of series XI which is non-mesomorphic and assume that all other homologues will also be non-mesomorphic (see series III). If the fluorine is present in a *meta*-position on the first phenyl ring, independent of whether it is an *n*-alkyl or *n*-alkoxy terminal chain, the derivatives are non-mesomorphic. A plot of the transition temperature as a function of the length of the terminal *n*-alkyl chain for series X is shown in figure 12 and the B_2 –I transition points show the usual behaviour.

From these observations, it is very clear that for

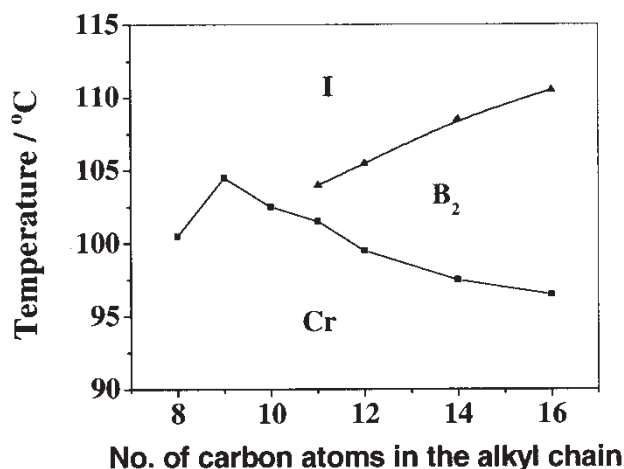


Figure 12. A plot of transition temperature as a function of terminal chain length for series X.

fluorine substitution at the *ortho*-position to the carbonyl group of either the middle or the outer phenyl rings, the mesomorphic behaviour observed in the parent series of compounds is retained with minimal changes. However, the effect is dramatic when a fluorine

is substituted in the *meta*-position of the middle or the outer phenyl rings. In many cases (series III, VIII, IX and XI), fluorine substitution completely destroys the mesophase and in some other cases (series V and VII) the switching behaviour, as well as the structure, of the mesophase is completely changed when compared with the unsubstituted compounds.

3.2. X-ray investigations

The mesomorphic behaviour including XRD studies have been reported [25] for series I, II and III. Compounds of series I and II exhibit B_6 , B_1 and B_2 mesophases on ascending the series. However, in series III only one homologue (compound 32) is mesomorphic, showing a metastable B_6 phase. The remaining homologues are non-mesomorphic.

The XRD studies carried out on the mesophases of the compounds of the various other series considered here are described below. The XRD values obtained for some of the mesophases of these compounds are summarized in table 11. In series IV, compound 43 shows two sharp reflections in the small angle region at

Table 11. The spacings (\AA) obtained for different mesophases and the corresponding Miller indices shown in brackets for various compounds under investigation. The XRD studies have been carried out on mesophases obtained on cooling the isotropic phases.

| Compound | d -spacings/ \AA (Miller indices) | Lattice parameters/ \AA | | Phase type |
|----------|--|----------------------------------|------|------------|
| | | a | b | |
| 4 | 18.0 (01), 9.0 (02) | — | — | B_6 |
| 8 | 24.7 (11), 21.1 (02) | 30.5 | 42.2 | B_1 |
| 12 | 35.7 (01), 17.9 (02) | — | — | B_2 |
| 18 | 17.2 (01), 8.6 (02) | — | — | B_6 |
| 19 | 17.9 (01) | — | — | B_6 |
| 21 | 20.5 (11), 19.2 (02) | 24.2 | 38.4 | B_1 |
| 23 | 23.7 (11), 20.9 (02) | 28.8 | 41.8 | B_1 |
| 27 | 33.0 (01), 16.5 (02) | — | — | B_2 |
| 43 | 19.5 (01), 9.7 (02) | — | — | B_6 |
| 44 | 21.8 (11), 20.5 (02) | 25.7 | 41.0 | B_1 |
| 49 | 33.7 (01), 16.8 (02) | — | — | B_2 |
| 50 | 36.3 (01), 18.5 (02), 12.3 (03) | — | — | B_2 |
| 57 | 39.2 (01), 19.6 (02), 13.0 (03) | — | — | B_{X1} |
| 58 | 42.3 (01), 21.3 (02), 14.2 (03) | — | — | B_{X1} |
| 59 | 45.3 (01), 22.7 (02), 15.1 (03) | — | — | B_{X1} |
| 60 | 46.7, 26.6, 17.8, 15.9 | — | — | B_{X2} |
| 61 | 49.7, 24.8, 18.7, 16.6 | — | — | B_{X2} |
| 65 | 17.9 (01), 9.0 (02) | — | — | B_6 |
| 67 | 19.8 (11), 19.2 (02) | 23.1 | 38.4 | B_1 |
| 73 | 33.0 (01), 16.5 (02) | — | — | B_2 |
| 74 | 35.3 (01), 17.8 (02), 11.9 (03) | — | — | B_2 |
| 75 | 37.4 (01), 12.6 (03) | — | — | B_2 |
| 77 | 17.9 (01), 8.9 (02) | — | — | B_6 |
| 80 | 24.6 (11), 20.0 (02) | 31.2 | 40.0 | B_1 |
| 82 | 35.6 (01), 17.8 (02) | — | — | B_{X1} |
| 85 | 38.7 (01), 19.4 (02) | — | — | B_{X1} |
| 86 | 41.6 (01), 20.9 (02), 13.9 (03) | — | — | B_{X1} |
| 100 | 39.8 (01), 19.9 (02), 13.3 (03), 10.0 (04) | — | — | B_2 |

$d_1=19.5\text{ \AA}$ and $d_2=9.7\text{ \AA}$ at a temperature of 118°C . These reflections are in the ratio 1:1/2 indicating a lamellar ordering in the mesophase. However, the first order reflection at 19.5 \AA can be indexed to a reflection from (0 1) plane which corresponds to nearly half the molecular length by assuming a fully extended all *trans*-conformation of the alkoxy chain. This clearly shows intercalation as well as tilting of the bent-core molecules in the mesophase. Also, a diffuse peak in the wide angle region at 4.7 \AA shows the absence of an in-plane order. Although the mesophase shows a focal-conic texture, it cannot be aligned homeotropically and hence the possibility of a SmA phase can safely be eliminated. In addition, the mesophase cannot be switched electro-optically. From all these observations, we have concluded that this mesophase is indeed a B_6 . The X-ray angular intensity profile obtained for the mesophase of compound **43** is shown in figure 13. Similar XRD patterns were obtained for the B_6 phase of other homologous series and are shown in table 11. Since the B_6 phase obtained for shorter chain lengths of compounds under investigation, the probability of the chains taking different conformations is small. The estimated tilt angle of the molecules is of the order of $25\text{--}30^\circ$ depending upon the chemical structure of the compounds.

The XRD pattern of an unoriented sample of compound **44** shows two sharp reflections at $d_1=21.8\text{ \AA}$ and $d_2=20.5\text{ \AA}$ in the small angle region at 109°C (monotropic phase). These could be indexed as reflections from (1 1) and (0 2) planes, forming a rectangular lattice with lattice parameters $a=25.7\text{ \AA}$ and $b=41\text{ \AA}$ by assuming a tilt of the molecules. As usual, a diffuse peak in the wide angle region at about 4.6 \AA was obtained which is indicative of a liquid-like in-plane

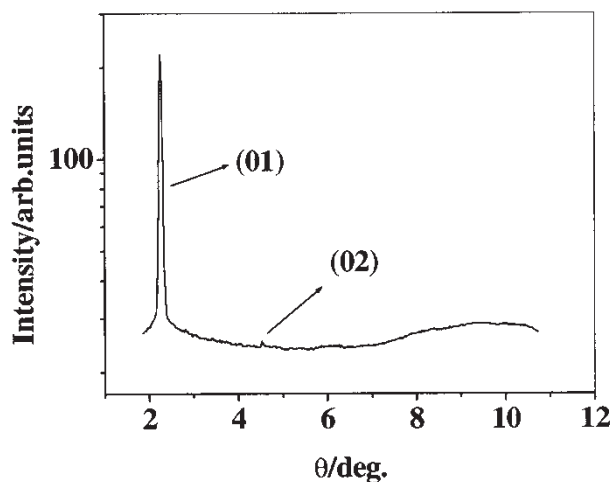


Figure 13. X-ray angular intensity profile obtained for the B_6 mesophase of compound **43**.

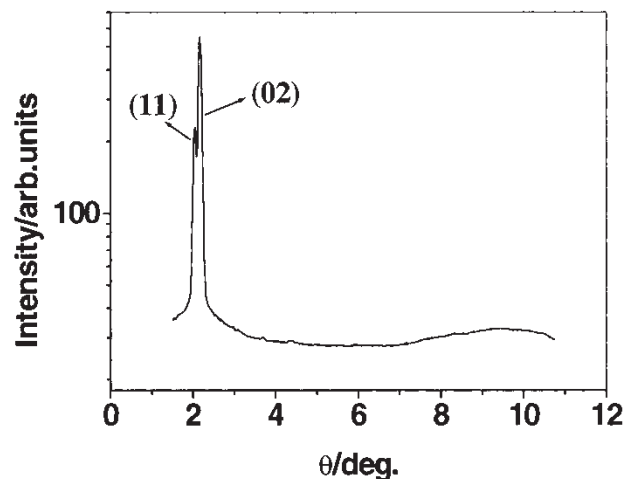


Figure 14. X-ray angular intensity profile obtained for the B_1 mesophase of compound **44**.

order. The X-ray angular intensity profile obtained for the mesophase of compound **44** is shown in figure 14. We have also obtained a monodomain sample for the B_1 phase of compound **80**. The pattern observed in the small angle region of this sample is shown in figure 15. The innermost four spots obtained are from two-dimensional (1 1) planes and the outer two spots are due to the intercalated layered planes (0 2). No electro-optical switching is observed for this mesophase even at fairly high electric fields. From XRD studies and textural features we have identified this mesophase to be a two-dimensional B_1 phase. Based on XRD patterns and optical textures the mesophases of compounds **67–69** of series VI as well as compound **79** of series VII, have all been characterized as a B_1 phase.

The mesophase of the higher homologues of series IV showed a different XRD pattern. For example, in the small angle region, compound **50** showed equally spaced

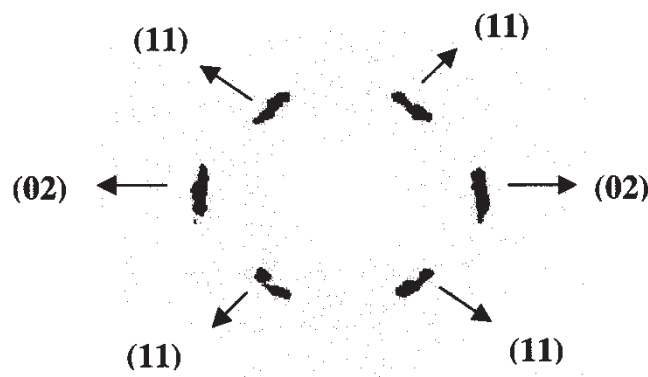


Figure 15. The small angle oriented pattern of the columnar B_1 phase obtained for compound **80**. The inner four spots obtained are due to the two-dimensional (1 1) planes and the outer two spots are from the intercalated layer planes (0 2).

Bragg reflections at $d_1=36.3\text{ \AA}$, $d_2=18.5\text{ \AA}$ and $d_3=12.3\text{ \AA}$, indicating a lamellar ordering in the mesophase. The first order layer spacing is lower than the calculated molecular length suggesting that this is a tilted smectic phase with a calculated tilt angle of about 53° . As normally observed a diffuse wide angle reflection at 4.7 \AA could also be seen, indicating a liquid-like in-plane order. The X-ray angular intensity profile obtained for the mesophase of compound **50** is shown in figure 16. The mesophase shows antiferroelectric switching behaviour and exhibits all the textural features of a B_2 phase. Hence, we have characterized this mesophase as B_2 . Similar XRD patterns and electro-optical switching characteristics were obtained for compounds **71–76** of series VI and compounds **97–100** of series X and all have been assigned as a B_2 phase.

The detailed XRD studies for the mesophases of the compounds of series V have already been reported [21]. Compounds **57–59** show a lamellar structure (B_{X1} phase) while compounds **60** and **61** show a two-dimensional structural pattern (B_{X2}), and as reported both exhibit ferroelectric properties. As can be seen in table 11, the layer thickness in the B_{X1} phase increases on increasing the chain length (42.3 \AA for compound **58** and 45.3 \AA for compound **59**), as is usual for any smectic phase. However, the increase in layer thickness appears to be maintained even in the two-dimensional B_{X2} phase of compounds **60** and **61** (46.7 \AA for compound **60** and 49.7 \AA for compound **61**). The XRD pattern for the higher homologues (compounds **82–89**) of series VII shows the following features. Compound **86** shows a diffuse peak at 4.7 \AA in the wide angle region indicating a liquid-like in-plane order; in the small angle region, reflections at $d_1=41.6\text{ \AA}$, $d_2=20.9\text{ \AA}$ and $d_3=13.9\text{ \AA}$ were obtained at 110°C . These reflections are indicative of a lamellar ordering in the mesophase with a tilt angle

of about 47° . The layer spacing obtained for this mesophase is independent of temperature. The X-ray intensity profile obtained for the mesophase of this compound is shown in figure 17. As we shall see later, the mesophase exhibits ferroelectric properties and we have assigned the symbol B_{X1} to the phase.

The XRD patterns of compounds **90–93** and **101** show many sharp reflections in the small angle as well as wide angle regions, indicating the crystalline nature of these compounds.

From the XRD studies of various compounds, the data of which are recorded in table 11, the following observations can be made. Depending on the position of fluorine in these series of compounds, both ferro- and antiferro-electric phases are obtained. The layer thicknesses vary from series to series for homologues with the same chain length. For example, the unsubstituted parent compound **12** (series I, $n=12$) has a layer thickness of 35.7 \AA while the corresponding fluorine-substituted compounds exhibit the following layer spacings: compound **27** (series II, $n=12$), 33 \AA ; compound **49** (series IV, $n=12$), 33.7 \AA ; compound **57** (series V, $n=12$), 39.2 \AA ; compound **73** (series VI, $n=12$), 33 \AA ; compound **85** (series VII, $n=12$), 38.7 \AA . It is clear that if a fluorine is substituted in an *ortho*-position either on the middle or the outer phenyl rings or on both phenyl rings, then the layer spacings obtained are lower than the value obtained for the unsubstituted parent compounds of the same homologue. However, if the fluorine is substituted in a *meta*-position on the outer phenyl ring then the layer spacing increases when compared with the parent compounds.

As reported by Bedel *et al.* [19] fluorine substitution in the *ortho*-position with respect to the carbonyl group of the outer phenyl ring in five-ring Schiff's base esters

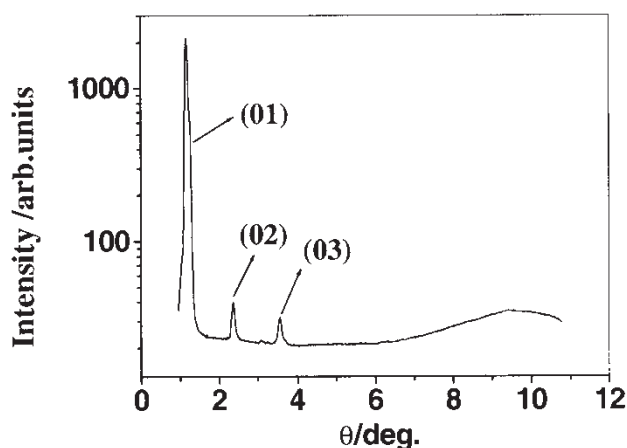


Figure 16. X-ray angular intensity profile obtained for the B_2 mesophase of compound **50**.

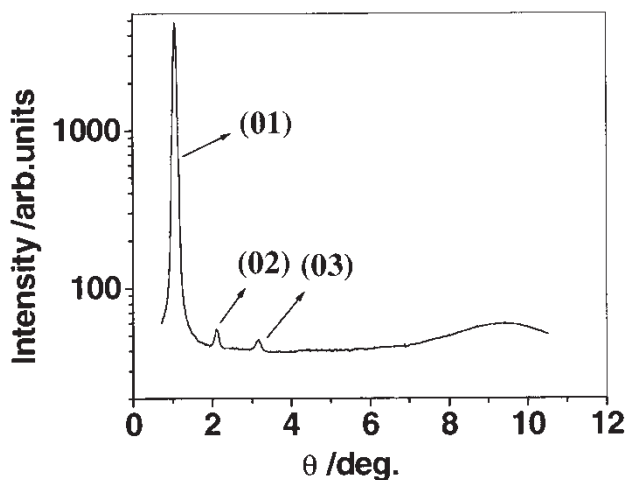


Figure 17. X-ray angular intensity profile obtained for the B_{X1} mesophase of compound **86**.

reduces the layer spacing of the B_2 phase when compared with the unsubstituted parent compounds. They have also speculated that this may be due to the large inter-layer penetration of the terminal chains. This kind of inter-layer interaction of terminal chains is entropically favourable for the antiferroelectric ordering of BC molecules in successive layers (B_2 phase) [20]. This may also explain the occurrence of favourable sequence B_6 , B_1 and B_2 phases on ascending the series. However, if a fluorine substitution is in the *ortho*-position with respect to the terminal chain of the outer phenyl ring (which gives rise to the ferroelectric ground state), these inter-layer interactions will be unfavourable, which also increases the layer spacing. Thus, the position of fluorine substitution strongly influences the electrostatic interactions as well as conformational changes, which results in the decrease or increase of the layer spacings (due to coupling or decoupling of layers, respectively).

3.3. Electro-optical studies

The electro-optical switching behaviour was investigated for several fluoro-substituted compounds belonging to different homologous series with a view to examining how the position of the fluorine substituent changes the switching behaviour. Obviously, the starting point for any such investigation would be to consider the mesomorphic behaviour and the switching characteristics of the unsubstituted parent compounds (series I). As reported earlier [25], compounds **1–5** show a B_6 phase and compounds **6–9** show a B_1 phase, and neither of these phases switch. However, compounds **10–15** exhibit the antiferroelectric B_2 phase [25, 26]. When a fluorine is substituted *ortho* to the carbonyl group of the middle phenyl ring (series II), the mesomorphic behaviour is similar to those of the parent compounds. However, in the case of compounds of series III, only one compound shows a monotropic B_6 phase and the remaining are non-mesomorphic. The switching characteristics of these two series (I and II) have already been reported [25].

Electro-optical switching experiments were carried out for one of the compounds of series IV in which there is fluorine substitution *meta* to the terminal *n*-alkoxy chain. A sample of compound **51** was taken in a cell constructed for homogeneous alignment with a thickness of $8.7\ \mu\text{m}$. On cooling from the isotropic phase under a d.c. electric field of about $3.5\ \text{V}\ \mu\text{m}^{-1}$ (threshold voltage is about $2.5\ \text{V}\ \mu\text{m}^{-1}$), colourful spherulitic growth could be observed under a polarizing microscope. The dark brushes seen make an angle with respect to the orientation directions of the crossed polarizers and by reversing the polarity of the electric field, the brushes rotate in the opposite direction.

However, on switching off the electric field the ferroelectric state is stabilized, revealing bistability. At a relatively higher electric field of about $7\ \text{V}\ \mu\text{m}^{-1}$ tristable switching is clearly seen under a polarizing microscope as shown in figure 18. The antiferroelectric ground state of this mesophase is further confirmed by a triangular wave method which will be described below. These observations indicate the existence of concentric circular smectic layers. The dark extinction cross shown in figure 18 indicates the position of the director of the bent-core molecules, is parallel or perpendicular to the crossed polarizers. As can be seen in figure 18, the switching ferroelectric domains are chiral, in which the antiferroelectric ground state must contain the anticlinic tilt of BC molecules in successive layers, and hence the resulting extinction cross is parallel to the crossed polarizers. On application of an electric field, the maximum rotation of the dark brushes obtained with respect to the layer normal is about $\pm 40^\circ$, which is the optical tilt angle.

To measure the spontaneous polarization of this switchable mesophase, the triangular wave method was employed. The same cell was also used for this experiment. By applying a fairly high triangular voltage of about $\pm 17\ \text{V}\ \mu\text{m}^{-1}$ at a frequency of 30 Hz at 95°C , two polarization current peaks are observed for each half-cycle, confirming the antiferroelectric ground state of this mesophase. A typical switching current response obtained in the B_2 phase of compound **51** is shown in figure 19. The calculated average saturated polarization value is about $440\ \text{nC}\ \text{cm}^{-2}$.

A similar antiferroelectric current response was obtained by the application of a modified triangular wave electric field for compound **75**. The saturated polarization value for the B_2 mesophase of this compound was determined to be $635\ \text{nC}\ \text{cm}^{-2}$; the current response trace obtained is shown in figure 20.

The detailed electro-optical switching behaviour of compounds of series V have already been reported [21]. Ferroelectric properties have been clearly demonstrated by both the triangular wave method and the bistability in smectic as well as the two-dimensional mesophases. The switching behaviour of compounds of series VII (compounds **82–89**) is similar to those observed in the B_{X1} phase of compounds **58** and **59** of series V. For example, on slow cooling from the isotropic phase of compound **86**, the mesophase appears dark but chiral domains of opposite handedness could be seen by rotating ($\approx 6^\circ$) either the polarizer or analyzer. An optical photomicrograph showing the heterochiral domains in the B_{X1} phase of compound **86** is shown in figure 21. On applying a triangular wave electric field of about $\pm 11\ \text{V}\ \mu\text{m}^{-1}$ (threshold voltage), these domains transform to a more birefringent texture as

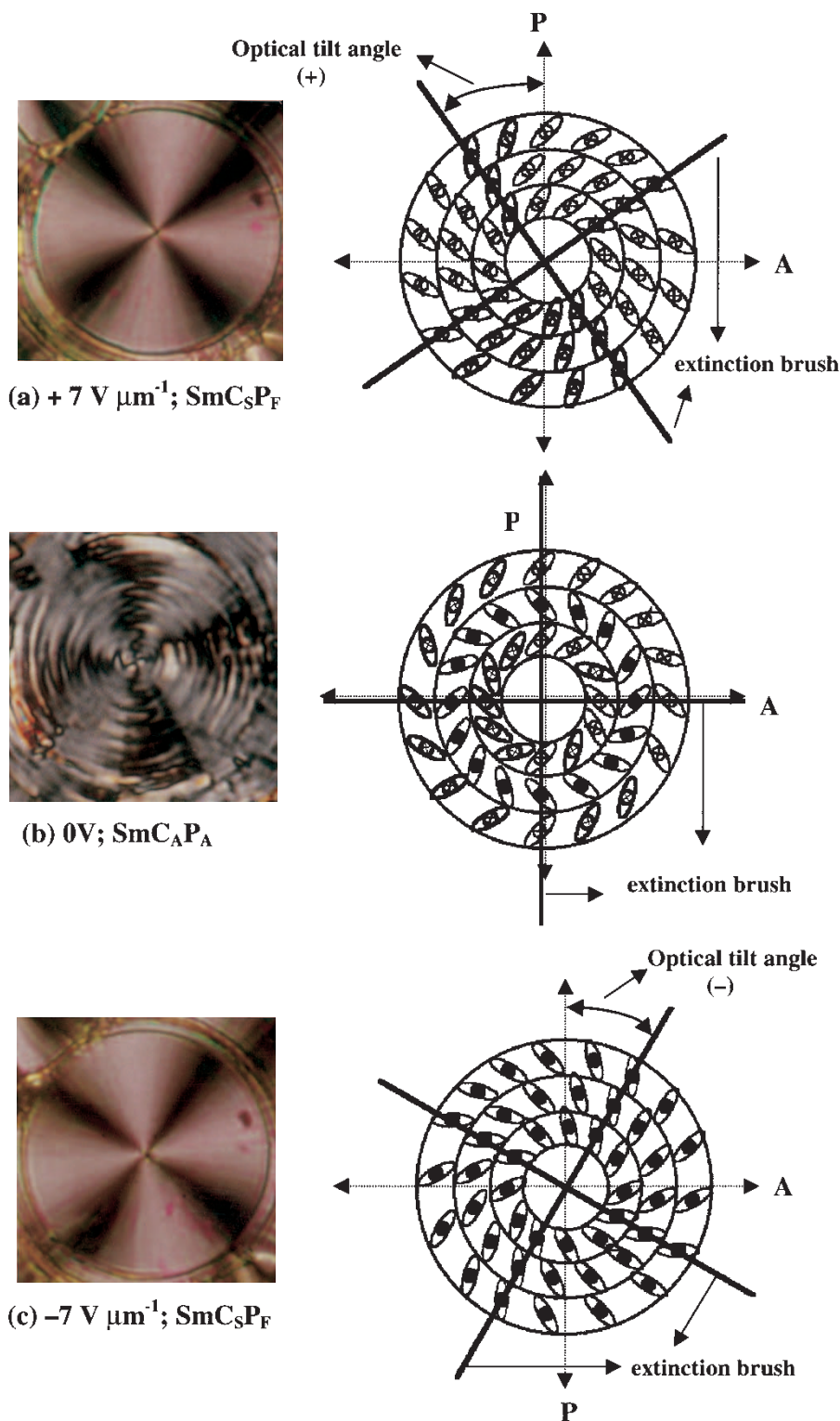


Figure 18. Optical photomicrograph of circular domains obtained for compound **51** under a d.c. electric field. (a) $+7 \text{ V } \mu\text{m}^{-1}$, chiral ferroelectric state (SmC_5P_F); (b) $0 \text{ V } \mu\text{m}^{-1}$, chiral antiferroelectric ground state (SmC_AP_A); (c) $-7 \text{ V } \mu\text{m}^{-1}$, another chiral ferroelectric state (SmC_5P_F) demonstrating the tristable switching for an antiferroelectric phase. On the right-hand side is shown a schematic representation of the arrangement of molecules in domains of concentric circular smectic layers, responsible for the occurrence of dark brushes in both ferro- and antiferro-electric states by the application of an electric field between crossed polarizers. The layer normal is along the direction of the polarizer.

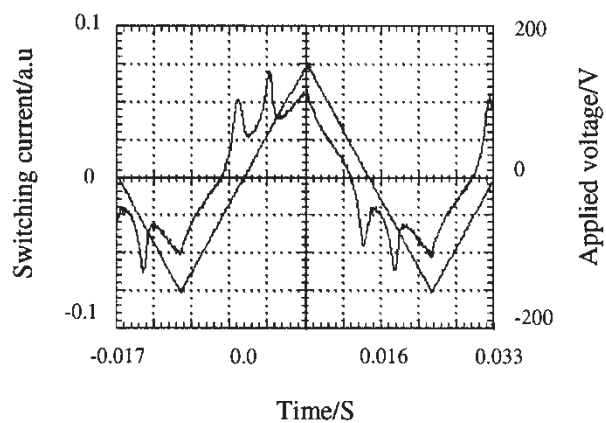


Figure 19. Switching current response obtained in the mesophase of compound **51** by applying a triangular voltage (± 148 V, 30 Hz) at 95°C ; sample thickness $8.7\ \mu\text{m}$; spontaneous polarization $440\ \text{nC cm}^{-2}$.

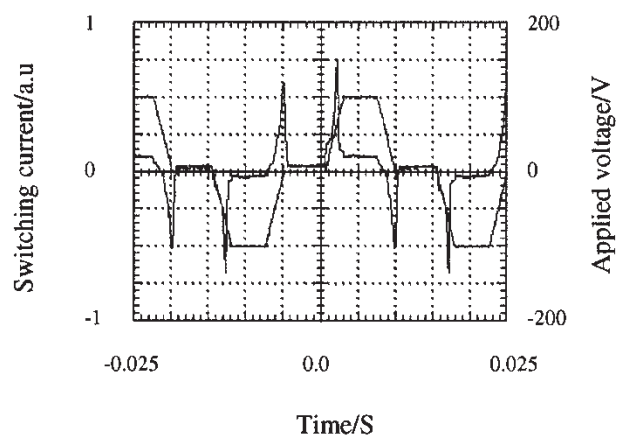


Figure 20. Switching current response obtained in the mesophase of compound **75** by applying a modified triangular voltage (± 100 V, 33 Hz) at 94°C ; sample thickness $6.2\ \mu\text{m}$; spontaneous polarization $P_s \sim 635\ \text{nC cm}^{-2}$.

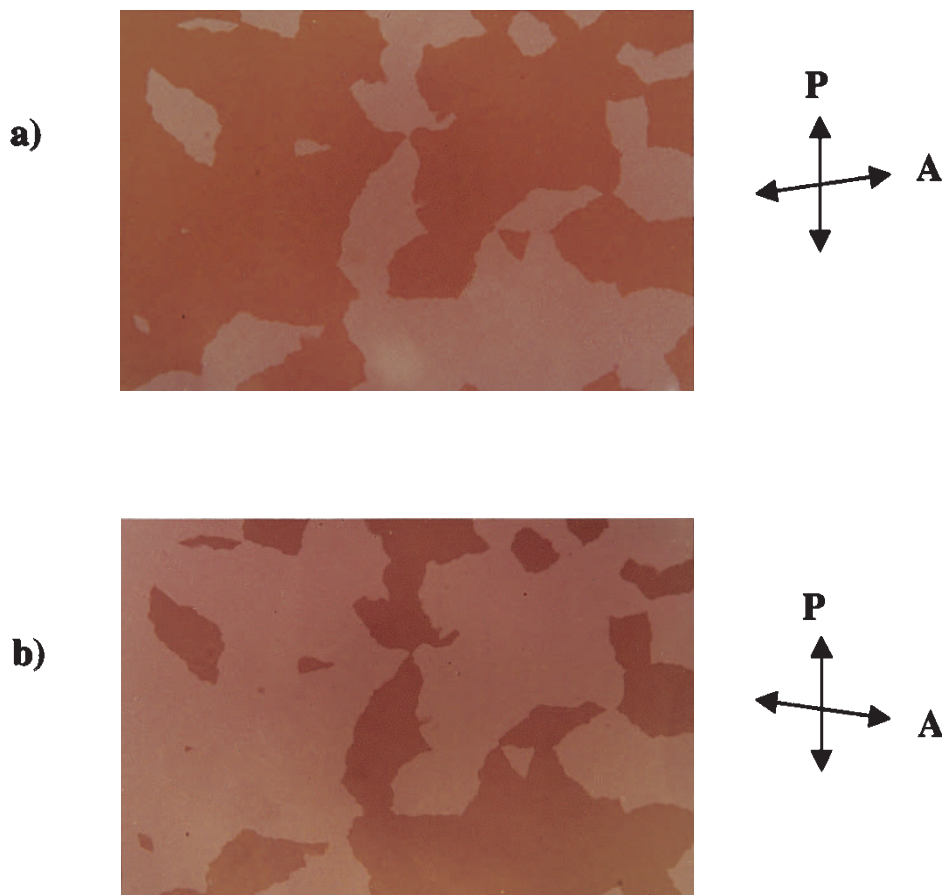


Figure 21. Optical photomicrograph of heterochiral domains obtained on cooling the B_{X1} mesophase of compound **86** and rotating the crossed polarizers ($\pm 6^\circ$).

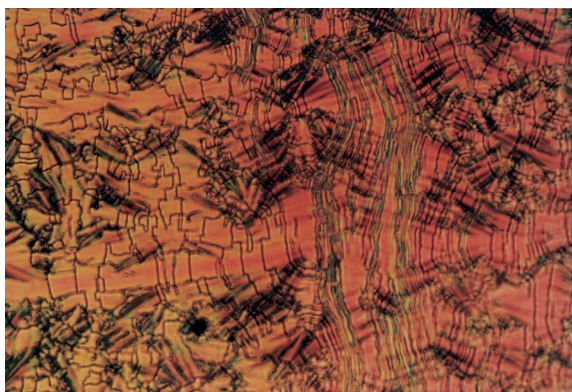


Figure 22. A photomicrograph of the texture obtained from the dark regions of the B_{X1} phase of compound **86** by the application of a triangular wave electric field.

shown in figure 22. Simultaneously, a single current peak was recorded for each half-cycle of the triangular wave which exists even at low frequencies (<1 Hz) indicating the ferroelectric nature of the mesophase. The saturated polarization at $\pm 13 \text{ V } \mu\text{m}^{-1}$ for this ferroelectric phase was determined to be about 280 nC cm^{-2} . A typical current response trace obtained for this mesophase is shown in figure 23. It should also be mentioned that on switching off the electric field, the colourful texture relaxes, in contrast to what was observed for the B_{X1} mesophase of compounds of series V. In addition, when a modified triangular wave electric field was applied to the sample, clearly only one current peak for each half-cycle was seen, supporting the ferroelectric nature of the mesophase. The modified triangular wave current response obtained for this B_{X1} phase is shown in figure 24.

In order unambiguously to establish ferroelectricity, a sample of compound **86** was taken in a $6 \mu\text{m}$ thick

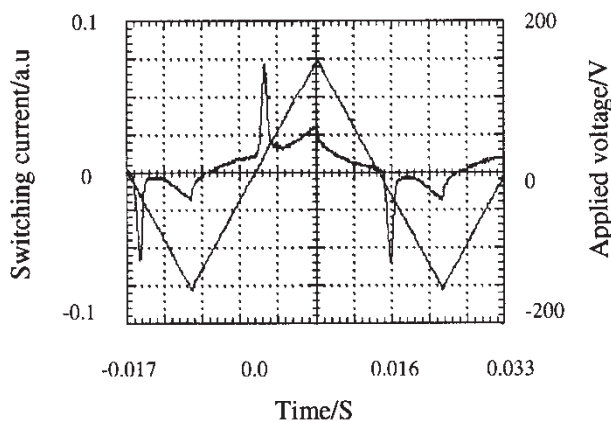


Figure 23. Switching current response obtained in the mesophase of compound **86** by applying a triangular voltage ($\pm 150 \text{ V}$, 30 Hz) at 110°C ; sample thickness $11.5 \mu\text{m}$; spontaneous polarization 280 nC cm^{-2} .

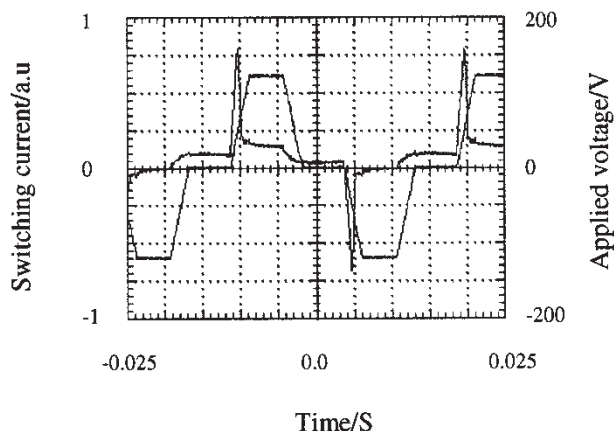


Figure 24. Switching current response obtained in the mesophase of compound **86** by applying a modified triangular voltage ($\pm 140 \text{ V}$, 33 Hz) at 110°C ; sample thickness $11.5 \mu\text{m}$.

cell prepared for homogeneous alignment. On slow cooling of the isotropic liquid under a d.c. electric field of $16 \text{ V } \mu\text{m}^{-1}$, partially aligned circular domains could be observed. When viewed under a polarizing microscope, it was seen that the dark brushes make an angle with respect to the crossed polarizers. On reversing the polarity of the field, the dark brushes rotate in the opposite direction. Interestingly, the orientation of the dark brushes is retained when the electric field is switched off thus proving bistability and hence the ferroelectric nature of the B_{X1} phase. Also, the texture remains unchanged on switching off the d.c. electric field. The calculated optical tilt angle in the ferroelectric B_{X1} phase is about $\pm 35^\circ$. The optical photomicrographs obtained in the states with and without the field are shown in figure 25.

4. Conclusions

A systematic study of the influence of fluorine substituents on the liquid crystalline properties of five-ring esters has been carried out. It is observed that the position of the fluorine plays a major role in influencing the type of mesophase formed. In one series (III), the mesomorphic properties are greatly suppressed. The most interesting result is the occurrence of two different ferroelectric phases, when a fluorine is substituted *ortho* to the terminal *n*-alkoxy chain (series V and VII). Also, whenever a ferroelectric phase is observed, the layer spacing is found to increase. However, in the case of fluorine-substituted compounds exhibiting an antiferroelectric phase, the layer spacing decreases. Surprisingly in such systems, the mesophase/s are destabilized if another fluorine is substituted in the *meta*-position of the middle phenyl ring (series IX). All these observations suggest that dipolar interactions play a significant

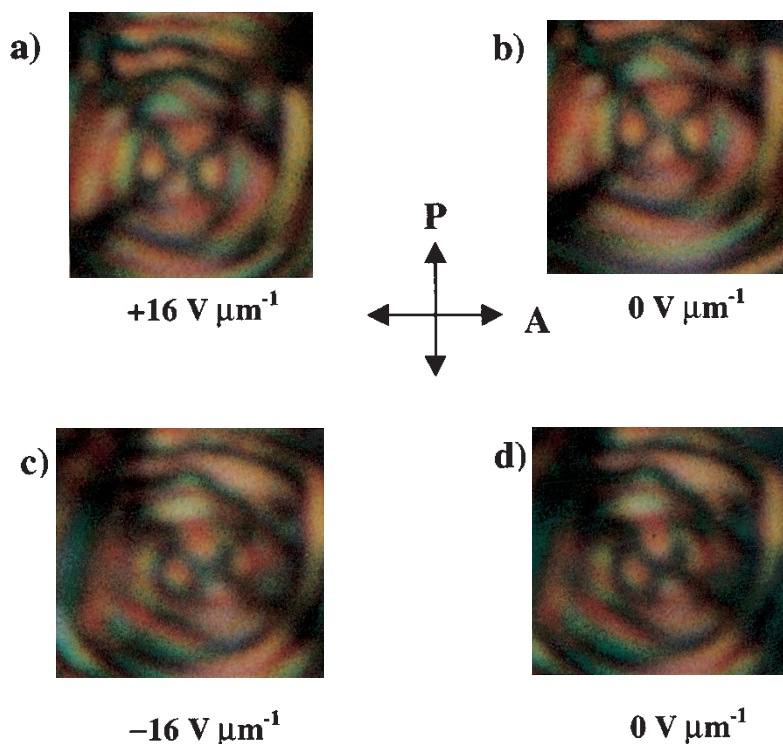


Figure 25. Optical photomicrographs of circular domains obtained for compound **86** under a d.c. electric field of about $\pm 16 \text{ V } \mu\text{m}^{-1}$. Domains (a) and (b) obtained at $+16 \text{ V } \mu\text{m}^{-1}$ and 0 V respectively. Similarly, domains (c) and (d) obtained after the reversal of the polarity of the applied field; that is, $-16 \text{ V } \mu\text{m}^{-1}$ and 0 V respectively. Note that there is no change in the orientation directions of the dark brushes obtained with and without fields. This demonstrates bistability for the ferroelectric ground state (SmC_SP_F).

role in influencing the occurrence of a particular type of mesophase in these five-ring esters.

The authors would like to thank Mr P. N. Ramachandra for synthesizing some intermediate compounds, Ms K. N. Vasudha for recording the infrared spectra and DSC thermograms, and the Sophisticated Instruments Facility, Indian Institute of Science, Bangalore for recording the ^1H and ^{13}C NMR spectra.

References

- [1] PELZL, G., DIELE, S., and WEISSFLOG, W., 1999, *Adv. Mat.*, **11**, 707.
- [2] WEISSFLOG, W., WIRTH, I., DIELE, S., PELZL, G., and SCHMALFUSS, H., 2001, *Liq. Cryst.*, **28**, 1603.
- [3] ROUILLON, J. C., MARCEROU, J. P., LAGUERRE, M., NGUYEN, H. T., and ACHARD, M. F., 2001, *J. mater. Chem.*, **11**, 2946.
- [4] PELZL, G., DIELE, S., GRANDE, S., JAKLI, A., LISCHKA, C., KRESSE, H., SCHMALFUSS, H., WIRTH, I., and WEISSFLOG, W., 1999, *Liq. Cryst.*, **26**, 401.
- [5] WEISSFLOG, W., LISCHKA, C., DIELE, S., PELZL, G., and WIRTH, I., 1999, *Mol. Cryst. liq. Cryst.*, **328**, 101.
- [6] WEISSFLOG, W., LISCHKA, CH., DIELE, S., PELZL, G., WIRTH, I., GRANDE, S., KRESSE, H., SCHMALFUSS, H., HARTUNG, H., and STETTLER, A., 1999, *Mol. Cryst. liq. Cryst.*, **333**, 203.
- [7] DIELE, S., GRANDE, S., KRUTH, H., LISCHKA, C., PELZL, G., WEISSFLOG, W., and WIRTH, I., 1998, *Ferroelectrics*, **212**, 169.
- [8] PELZL, G., DIELE, S., JAKLI, A., LISCHKA, C., WIRTH, I., and WEISSFLOG, W., 1999, *Liq. Cryst.*, **26**, 135.
- [9] WEISSFLOG, W., LISCHKA, C., BENNE, I., SCHARF, T., PELZL, G., DIELE, S., and KRUTH, H., 1998, *Proc. SPIE*, **3319**, 14.
- [10] WIRTH, I., DIELE, S., EREMIN, A., PELZL, G., GRANDE, S., KOVALENKO, L., PANCENKO, N., and WEISSFLOG, W., 2001, *J. mater. Chem.*, **11**, 1642.
- [11] JAKLI, A., LISCHKA, CH., WEISSFLOG, W., PELZL, G., and SAUPE, A., 2000, *Liq. Cryst.*, **27**, 1405.
- [12] DEHNE, H., POTTER, M., SOKOLOWSKI, S., WEISSFLOG, W., DIELE, S., PELZL, G., WIRTH, I., KRESSE, H., SCHMALFUSS, H., and GRANDE, S., 2001, *Liq. Cryst.*, **28**, 1269.
- [13] MATRASZEK, J., MIECZKOWSKI, J., SZYDŁOWSKA, J., and GORECKA, E., 2000, *Liq. Cryst.*, **27**, 429.
- [14] LEE, C. K., and CHIEN, L. C., 1999, *Liq. Cryst.*, **26**, 609.
- [15] LEE, C. K., and CHIEN, L. C., 2000, *Ferroelectrics*, **243**, 231.
- [16] HEPPKE, G., PARGHI, D. D., and SAWADE, H., 2000, *Ferroelectrics*, **243**, 269.

- [17] NGUYEN, H. T., ROUILLON, J. C., MARCEROU, J. P., BEDEL, J. P., BAROIS, P., and SARMENTO, S., 1999, *Mol. Cryst. liq. Cryst.*, **328**, 177.
- [18] BEDEL, J. P., ROUILLON, J. C., MARCEROU, J. P., LAGUERRE, M., NGUYEN, H. T., and ACHARD, M. F., 2000, *Liq. Cryst.*, **27**, 1411.
- [19] BEDEL, J. P., ROUILLON, J. C., MARCEROU, J. P., LAGUERRE, M., NGUYEN, H. T., and ACHARD, M. F., 2002, *J. mater. Chem.*, **12**, 2214.
- [20] NADASI, H., WEISSFLOG, W., EREMIN, A., PELZL, G., DIELE, S., DAS, B., and GRANDE, S., 2002, *J. mater. Chem.*, **12**, 1316.
- [21] AMARANATHA REDDY, R., and SADASHIVA, B. K., 2002, *J. mater. Chem.*, **12**, 1.
- [22] RAUCH, S., BAULT, P., SAWADE, H., HEPPKE, G., NAIR, G. G., and JAKLI, A. *Phys. Rev. E.*, 2002, **66**, 021706.
- [23] AMARANATHA REDDY, R., and SADASHIVA, B. K., 2000, *Liq. Cryst.*, **27**, 1613.
- [24] GRAY, G. W., HOGG, C., and LACEY, D., 1981, *Mol. Cryst. liq. Cryst.*, **67**, 1.
- [25] (a) AMARANATHA REDDY, R., and SADASHIVA, B. K., 2003, "Materials Research: Current Scenario and Future Projections", edited by R. Chidambaram, 157; (b) SHUBASHREE, S., SADASHIVA, B. K., and SURAJIT DHARA., 2002, *Liq. Cryst.*, **29**, 789.
- [26] SHEN, D., PEGENAU, A., DIELE, S., WIRTH, I., and TSCHERSKE, C., 2000, *J. Am. chem. Soc.*, **122**, 1593.
- [27] SADASHIVA, B. K., RAGHUNATHAN, V. A., and PRATIBHA, R., 2000, *Ferroelectrics*, **243**, 249.